

# Superdiffusion and time-dependent long-range interactions on networks

Alfonso Allen-Perkins\*

*Complex System Group, Universidad Politécnica de Madrid, 28040-Madrid, Spain.  
Instituto de Física, Universidade Federal da Bahia, 40210-210 Salvador, Brazil.*

Alfredo Blanco Serrano†

*Instituto de Física, Universidade Federal da Bahia, 40210-210 Salvador, Brazil.*

Thiago Albuquerque de Assis‡

*Complex System Group, Universidad Politécnica de Madrid, 28040-Madrid, Spain.  
Instituto de Física, Universidade Federal da Bahia, 40210-210 Salvador, Brazil.*

Juan Manuel Pastor§

*Complex System Group, Universidad Politécnica de Madrid, 28040-Madrid, Spain.  
E.T.S.I.A.A.B, Universidad Politécnica de Madrid,  
Avd. Puerta de Hierro 4, 28040-Madrid, Spain.*

Ernesto Estrada¶

*Department of Mathematics and Statistics,  
University of Strathclyde, Glasgow, G1 1XQ, U.K.*

Roberto F. S. Andrade\*\*

*Instituto de Física, Universidade Federal da Bahia, 40210-210 Salvador, Brazil.*

(Dated: December 14, 2024)

## Abstract

This work addresses the motion of a random walker on a discrete structure with the presence of long-range interactions, the strength of which can change in time. No restriction is made on the nature of the substrate, which may range from ordered lattice to complex network. The presence of long-range interactions on regular lattices with nearest-neighbor hops enhances the speed of the diffusive motion, but the dependence of the mean square displacement (MSD) traveled by the walker has been found to still increase linearly with time. In contrast to this, our results for a model where strength of long range interactions increases with time reveals a non linear dependence of MSD with respect to time. The time duration of such a dependence, as well as the value of power law exponent, depend on the way the interactions change in time. The model on the cycle graph is amenable to exact analytical treatment within the Markov chain framework. Numerical simulations are in excellent agreement with the theoretical predictions, and can be easily extended to complex structures where analytical approaches are not possible.

---

\* alfonso.allen@hotmail.com

† alfredoblancoherrero@gmail.com

‡ thiagoaa@ufba.br

§ juanmanuel.pastor@upm.es

¶ ernesto.estrada@strath.ac.uk

\*\* randrade@ufba.br

## I. INTRODUCTION

In real-world complex systems many dynamical processes occur in discrete spaces. They include diffusion processes, synchronization of agents, epidemic spreading, and many others taking place in ecological, social, economic as well as infrastructural and technological systems [1]. Those systems can be represented by networks in which the nodes represent the entities of the system and the edges represent the interactions between such entities. Dynamical processes on these networks usually adopt a nearest-neighbor strategy of transferring “information” from one node to another. Here, random walk models have widespread use in the analysis of the diffusion of information and navigability on these networks as well as in the exploration of their structures to detect their fine-grained organization [2, 3].

Currently, it is well-documented that there are dynamical processes both in continuum and discrete spaces which do not follow this “nearest-neighbor paradigm”. For instance, self-diffusive processes of atoms and molecules adsorbed on metals display significant contributions due to jumps spanning more distant atoms in the metallic surface. The role of long-jumps in ad-atoms and molecules diffusing on metallic surface has been both theoretically and experimentally confirmed in many different systems [4–7]. In the continuum space, the use of random walks with Lévy flights is widely documented to model a large variety of processes in which long-range jumps occurs together with short-range ones, as in the motion of species in a given environment [8–11]. Another useful approach to study such processes is to consider fractionary differential equations [12] or non-linear diffusion equations [13]. More recently, another approach has emerged as an alternative to study dynamical processes on discrete spaces which combine nearest- and non-nearest-neighbors hops in an elegant mathematical way. This approach is based on the so-called  $d$ -path Laplacian operators which represent a natural generalization of the Laplacian operator on graphs [14, 15]. It has been employed to analyze consensus spreading or synchronization, among other phenomena [16–18].

In all quoted studies both in the continuum and discrete spaces, the laws governing the short and long-range hops of the diffusive particle remains constant in time. In the current work we address a different scenario in which such laws may change in time. Rather than being a simple mathematical digression, this problem is motivated by some real case scenarios, e.g., in networks where agents interact socially. Let us consider that people are

not only influenced by their direct acquaintances but also by certain indirect peers pressure. We can identify three naturally possible scenarios: (i) the indirect peers pressure remains constant in time; (ii) the indirect peers pressure decays with time and eventually disappears; (iii) the indirect peers pressure increases with time up to a certain level. The first scenario is the typical one treated in the literature using either of the three methods previously mentioned. The second scenario is represented by the fact that in the course of time such influence is no longer important, i.e., is not fashionable anymore and people are then mainly influenced by their direct acquaintances. This is the case, for instance, of smoking in Europe and USA in the last 10 years. People are no longer influenced indirectly by the fact that others smoke; only if your close friends or partners smoke you can be influenced by them. The last case could be paradigmatic of phenomena like “binge drinking” among teenagers in the UK [19]. Teenagers are not only influenced by their direct peers but also by the fact that currently it is fashionable to get drunk and social misbehave. This indirect peers pressure has been growing in time and became a new “fashion”. Then, the long-range influence of peers is no longer constant but increases with time until it eventually starts to decrease and disappears.

Taking into account the above discussion, in the current work we consider a model for diffusion of particles in a network, with short and long-range hops, in which the strength of the long range interactions changes in time. For this purpose, it is important to consider structures where the saturation effect, present in any finite system, occur after a sufficiently large time lapse, so that the role played by this extra feature in the different time scales of the diffusive process can be emphasized. Most used network types, like those generated within the Erdős-Rényi and Barabási-Albert frameworks, are characterized by short diameter, which favors saturation in a short time scale. Because of this, and also by the possibility of developing an exact analytical treatment of the dynamical properties, we restrict ourselves to the presentation of results for the large diameter cycle graphs. We focus our attention to the situation (iii) described above, in which the strength of the long-range interactions increases with time. As we will show, in this case, a very rich diffusive pattern emerges.

The paper is organized as follows. In Sec. II, we present the formalism used to describe random walks on complex networks with time-dependent long-range interactions (LRIs). The methodology employed to estimate the mean square displacement (MSD) on these type of networks is explained in Sec. III. Numerical results supporting the analytical expressions

for the time evolution of the MSD on cycle graphs with constant LRIs are shown in Sec. IV, whereas the findings for the time-dependent LRIs are explained in Sec. V. Our conclusions are summarized in Sec. VI. Finally, the deductions of the mathematical expressions used can be consulted in the appendices included at the end of this document.

## II. RANDOM WALKS ON NETWORKS WITH TIME-DEPENDENT LONG-RANGE INTERACTIONS

A *random walk* on the network  $G$  is a random sequence of vertices generated as follows: given a starting vertex  $i$  we select a neighbor  $j$  randomly, and move to this neighbor. Then we select a neighbor  $k$  of  $j$  randomly, and move to it, and so on [20, 21]. In this section we introduce the definitions and methodology to calculate the probability of finding a random walker at a given node of the graph at time  $t$ , when the random walker is initially located at node  $i$ .

Let  $G = (V, E)$  be a simple, undirected graph without self-loops. Let  $d_{ij}$  be the shortest path distance, that is, the number of edges in the shortest path connecting the nodes  $i$  and  $j$ , and let  $d_{max}$  be the graph diameter, that is, the maximum shortest path distance in the graph. Let us now define the  $d$ -path adjacency matrix [15] (or neighborhood adjacency matrix of order  $d$  [22]), denoted by  $\mathbf{A}_d$ , of a connected graph of  $N$  nodes as the square, symmetric,  $N \times N$  matrix whose entries are:

$$\mathbf{A}_d(i, j) = \begin{cases} 1 & \text{if } d_{ij} = d \\ 0 & \text{otherwise} \end{cases}, \quad (1)$$

where  $d \leq d_{max}$ .

Following [15], let us now consider the transformed  $d$ -path adjacency matrices of  $G$  given by:

$$\hat{\mathbf{A}}^\tau = \begin{cases} \sum_{d=1}^{d_{max}} d^{-s} \mathbf{A}_d & \text{if } \tau = \text{Mellin} \\ \mathbf{A}_1 + \sum_{d=2}^{d_{max}} e^{-\lambda d} \mathbf{A}_d & \text{if } \tau = \text{Laplace} \end{cases}, \quad (2)$$

where  $\tau$  indicates the type of transformation,  $s \geq 0$  and  $\lambda \geq 0$ . In case of  $s = -1$  and  $\tau = \text{Mellin}$ ,  $\hat{\mathbf{A}}^\tau$  is equal to the neighborhood matrix as defined in [22].

If the transformation parameters  $s$  and  $\lambda$  depend on time (i.e.,  $s = s(t)$  and  $\lambda = \lambda(t)$ ), then the transformed  $d$ -path adjacency matrices of  $G$  are also conditioned by  $t$ :

$$\hat{\mathbf{A}}^\tau(t) = \hat{\mathbf{A}}_t^\tau = \begin{cases} \sum_{d=1}^{d_{max}} d^{-s(t)} \mathbf{A}_d & \text{if } \tau = \text{Mellin} \\ \mathbf{A}_1 + \sum_{d=2}^{d_{max}} e^{-\lambda(t)d} \mathbf{A}_d & \text{if } \tau = \text{Laplace} \end{cases}. \quad (3)$$

Following [15, 23], let us define the strength of a given node  $i$  of a transformed  $d$ -path graph, at time  $t$ , as:

$$\hat{s}_t^\tau(i) = \left( \hat{\mathbf{A}}_t^\tau \vec{1} \right)_i \quad (4)$$

where  $\vec{x}$  is an all-x vector.

Consequently, the probability that a particle staying at node  $i$  hops to the node  $j$ , at time  $t$ , is given by:

$$P_t^\tau(i, j) = \frac{\hat{\mathbf{A}}_t^\tau(i, j)}{\hat{s}_t^\tau(i)}. \quad (5)$$

Let us denote by  $\hat{\mathcal{S}}_t^\tau$  the diagonal matrix with  $\hat{\mathcal{S}}_t^\tau(i, i) = \hat{s}_t^\tau(i)$  and let us define the *transition matrix* for the random walk, at time  $t$ , as  $\mathcal{P}_t = \left( \hat{\mathcal{S}}_t^\tau \right)^{-1} \hat{\mathbf{A}}_t^\tau$ . According to this definition, it is possible to see that  $\mathcal{P}_t$  is a stochastic matrix. Then, the vector containing the probability of finding a random walker at a given node of the graph at time  $t+1$  is given by

$$\vec{p}_{t+1} = \mathcal{P}_t^T \vec{p}_t, \quad (6)$$

where  $\mathbf{X}^T$  stands for the transpose of matrix  $\mathbf{X}$ .

The vector  $\vec{p}_t$  depends on the initial position of the random walker. We denote by  $\vec{p}_{t,i}$  the vector containing the probability of finding a random walker at a given node of the graph at time  $t$ , when the random walker is initially located at node  $i$ . Therefore, it is possible to write the following expression:

$$\vec{p}_{t,i} = \mathcal{P}_{t-1}^T \cdots \mathcal{P}_0^T \vec{p}_{0,i} = \left( \prod_{\delta=0}^{t-1} \mathcal{P}_\delta^T \right) \vec{p}_{0,i}, \quad (7)$$

where  $(\vec{p}_{0,i})_j = 1$  if  $i = j$ , and 0 otherwise. If  $s$  (or  $\lambda$ ) is constant, then  $\mathcal{P}_t = \mathcal{P}$  and we recover the Markov chain formulation proposed in [15, 23].

### III. MSD ON NETWORKS WITH TIME-DEPENDENT LONG-RANGE INTERACTIONS

The MSD is a measure of the deviation time between the position of a particle,  $x(t)$ , and a reference position,  $x_0$ . In most cases, this quantity is described by an expression of the form:

$$\langle (x(t) - x_0)^2 \rangle = \langle r^2(t) \rangle \sim t^\gamma, \quad (8)$$

where the value of the parameter  $\gamma$  classifies the type of diffusion into normal diffusion ( $\gamma = 1$ ), subdiffusion ( $\gamma < 1$ ), or superdiffusion ( $\gamma > 1$ ).

The MSD has been studied on simple networks (i.e., unweighted graphs without self-loops) by means of random walkers [24, 25]. In this case, this quantity is a measure of the distance  $r$  covered by a typical walker after performing  $t$  steps.

#### A. The length of the shortest path between two nodes of a weighted graph

Since the  $d$ -path transformation of  $G = (V, E)$  defines a weighted topology (see Eqs. 2 and 3), in this work we extend the methodology to estimate MSD on simple graphs. To do so, we take into consideration the influence of the weights of the ties on the length of the shortest path between two nodes. Following [26], we assume that the weights  $\hat{\mathbf{A}}_t^\tau(i, j)$  are operationalizations of tie strength between the nodes  $i$  and  $j$ . Thus, the length of the shortest path between two nodes of a weighted graph  $G$ ,  $d_{i,j}^\alpha$ , can be formalized as:

$$d_{i,j}^\alpha = \min \left( \frac{1}{\left(\hat{\mathbf{A}}_t^\tau(i, h_1)\right)^\alpha} + \frac{1}{\left(\hat{\mathbf{A}}_t^\tau(h_1, h_2)\right)^\alpha} + \dots + \frac{1}{\left(\hat{\mathbf{A}}_t^\tau(h_\ell, j)\right)^\alpha} \right), \quad (9)$$

where  $h_1, h_2, \dots, h_\ell$  are intermediary nodes on a given path between node  $i$  and  $j$ ,  $\alpha$  is a nonnegative tuning parameter, and the minimum value is considered over all the possible paths. For  $\alpha < 1$ , a shorter path composed of weak connections is favored over a longer path with strong ties. On the contrary, when  $\alpha > 1$ , the impact of additional intermediary nodes is relatively unimportant compared to the strength of the connection. So, paths with more intermediaries are favored. When  $\alpha = 0$ , the outcome is the shortest path distance of an undirected and unweighted graph, whereas when  $\alpha = 1$ , the outcome is the one obtained

with Dijkstra's algorithm [27]. Note that with the previous method an infinite large distance would be assigned to absent ties (weight of 0).

Finally, it is worth mentioning that, according to Eqs. 2 and 3, all the elements of the  $d$ -path transformed adjacency matrix are less than or equal to one (i.e.,  $\hat{\mathbf{A}}_t^\tau(i, j) \leq 1$ ). Consequently, in case of  $\alpha \geq 1$ , the weighted shortest path distance between nodes  $i$  and  $j$ ,  $d_{i,j}^\alpha$ , is equal to the shortest path distance between those nodes when there are no LRIs (i.e.,  $d_{i,j}^\alpha = d_{i,j}$ ).

## B. MSD on weighted networks

Given an initial condition  $\vec{p}_{0,i}$ , we find the MSD of the random walker to the origin (i.e., the node  $i$ ), at each time step,  $r^2(t, i)$ . Let  $d_{i,j}^\alpha$  be the minimal distance from node  $j$  to the origin,  $i$ . Then,  $r^2(t, i)$  can be expressed as follows:

$$r^2(t, i) = \sum_{j=1}^N (d_{i,j}^\alpha)^2 (\vec{p}_{t,i})_j. \quad (10)$$

To calculate the MSD, we average over all the different initial positions of the walker:

$$\text{MSD} \equiv \langle r^2(t) \rangle = \frac{1}{N} \sum_{i=1}^N r^2(t, i) = \frac{1}{N} \sum_{i=1}^N \sum_{j=1}^N (d_{i,j}^\alpha)^2 (\vec{p}_{t,i})_j. \quad (11)$$

As can be observed, the estimation of MSD on networks with long-range interactions depends on various factors, namely: the discrete time-step  $t$ , the  $d$ -path transformation used  $\tau$  (Mellin or Laplace), the weight of the  $d$ -path transformation ( $s$  or  $\lambda$ ), the topology of  $G$ , and the tuning parameter of the shortest path length,  $\alpha$ . When the long-range interactions also depend on time, MSD is also conditioned by the time evolution of the weight of the  $d$ -path transformation ( $s(t)$  or  $\lambda(t)$ ). For the sake of simplicity, in this work we consider  $\tau = \text{Mellin}$  and  $\alpha \geq 1$  (i.e.,  $d_{i,j}^\alpha = d_{i,j}$ ).

## IV. TIME EVOLUTION OF THE MSD ON CYCLE GRAPHS WITH CONSTANT LRIS

In case of a cycle graph with  $N$  nodes, when we consider  $s = \infty$  for every  $t$  (i.e., the cycle graph has no LRIs) and  $N$  is an odd number, the MSD is given by:

$$\langle r^2(t) \rangle = \frac{N^2 - 1}{12} + \sum_{k=2}^{(N+1)/2} \cos^t(\theta_k) \frac{(-1)^{k+1}}{2 \sin(\frac{\theta_k}{2})} \cot\left(\frac{\theta_k}{2}\right), \quad (12)$$

where  $\theta_k \equiv \frac{2\pi}{N}(k-1)$  (see Appendix B for the deduction of Eq. 12).

Generally, when the Mellin transformation is used, for a constant  $s \leq \infty$  and  $\alpha \geq 1$ , the MSD can be approximated as:

$$\langle r^2(t) \rangle \approx \frac{N^2 - 1}{12} + \sum_{k=2}^{(N+1)/2} \left( 1 + 2 \frac{H_{0, \frac{N-1}{2}}^{(s-2)}}{H_{0, \frac{N-1}{2}}^{(s)}} \left( \frac{\pi(N-1)}{2N} \right)^2 \right)^t \frac{(-1)^{k+1}}{2 \sin(\frac{\theta_k}{2})} \cot\left(\frac{\theta_k}{2}\right). \quad (13)$$

Here  $H_{c,n}^{(m)}$  is the generalized harmonic number for nonnegative  $n$ , complex order  $m$  and complex offset  $c$  [28], defined as

$$H_{c,n}^{(m)} = \sum_{k=1}^n \frac{1}{(c+k)^m} \quad (14)$$

(see Appendix B for the deduction of Eq. 13).

The numeric estimation of Eq. 11 on cycle graphs with constant LRIs shows that it is possible to write the following approximation for Eq. 13:

$$\langle r^2(t) \rangle = \begin{cases} \langle r^2(1) \rangle t & \text{if } 1 \leq t \ll t_x \\ \langle r^2 \rangle_{\text{sat}} & \text{if } t \gg t_x \end{cases}, \quad (15)$$

where

$$\langle r^2 \rangle_{\text{sat}} = \frac{N^2 - 1}{12}, \quad (16)$$

$$\langle r^2(1) \rangle = \frac{\sum_{k=1}^{(N-1)/2} \left( \frac{N+1}{2} - k \right)^{2-s}}{\sum_{k=1}^{(N-1)/2} k^{-s}} = (-1)^{s-2} \frac{H_{-\frac{N+1}{2}, \frac{N-1}{2}}^{(s-2)}}{H_{0, \frac{N-1}{2}}^{(s)}}, \quad (17)$$

and

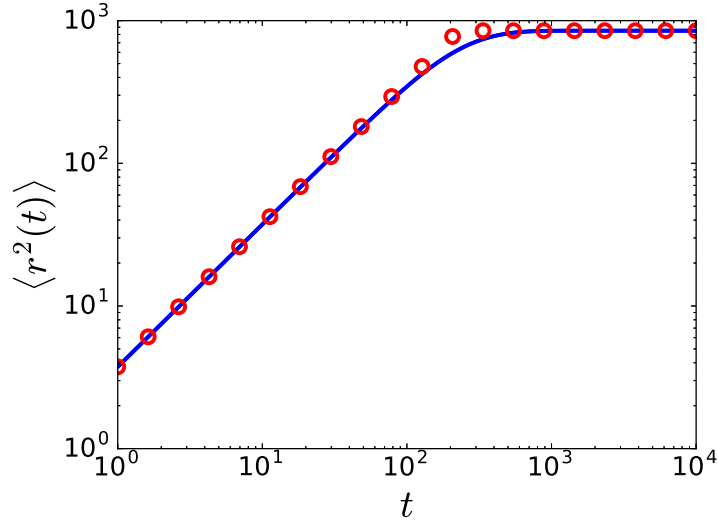


FIG. 1: Time evolution of MSD and of Eq. 15 for a cycle graph with  $N = 101$  nodes,  $s = 3$  and  $\alpha = 1.5$ .

$$t_x = \frac{\langle r^2 \rangle_{\text{sat}}}{\langle r^2(1) \rangle}, \quad (18)$$

represents the crossover time between the growth and saturation regimes (see Appendix B). Note that in case of  $s = \infty$ ,  $\langle r^2(1) \rangle = 1$ .

According to Eq. 15, the MSD on cycle graphs with constant LRIs exhibits a normal diffusion ( $\gamma = 1$ ) before saturation takes place (i.e., for  $t < t_x$ ). In fact, it is possible to obtain an universal curve for MSD on cycle graphs. In Fig. 2, we show the collapse of the MSD curves obtained for various cycle graphs, using different values of  $N$  and  $s$ . As can be observed, the slope of the universal curve is equal to 1, for  $t \ll t_x$ .

## V. TIME EVOLUTION OF THE MSD ON CYCLE GRAPHS WITH TIME-DEPENDENT LRIS

When LRIs depend on time (i.e.,  $s = s(t)$ ), and we consider the same assumptions used in the previous section (Mellin transform,  $\alpha \geq 1$ , and a cycle graph with an odd number of nodes  $N$ ), the expression for MSD can be approximated by:

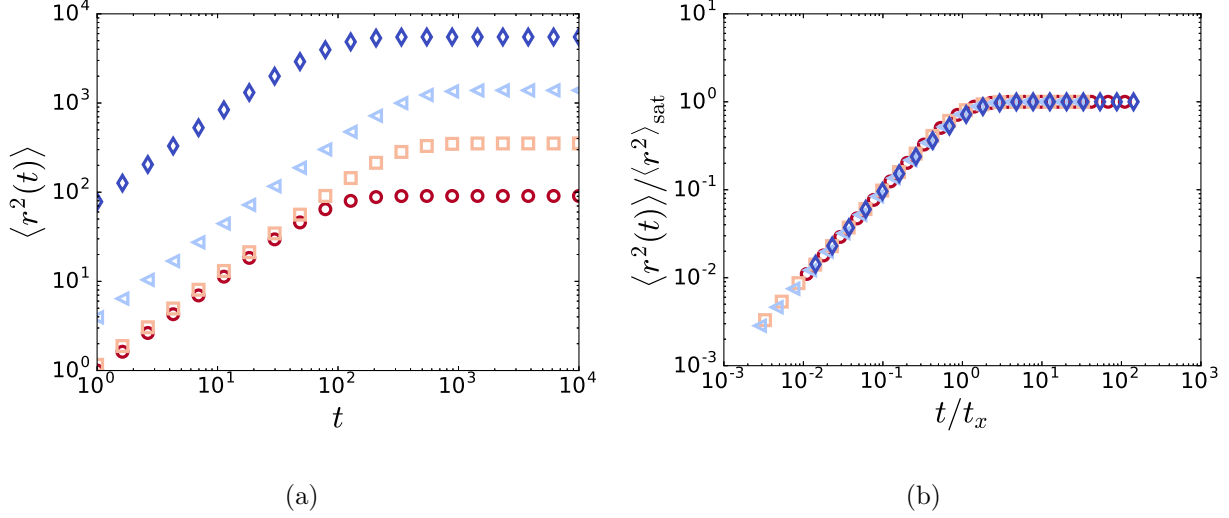


FIG. 2: (a) Left panel: Time evolution of the MSD for a cycle graph when  $N = 33$  and  $s = \infty$  (red circles),  $N = 65$  and  $s = 5$  (orange squares),  $N = 129$  and  $s = 3$  (cyan triangles), and  $N = 257$  and  $s = 2$  (blue rhombuses), when  $\alpha = 1.5$ . (b) Right panel: Collapse of the prior curves.

$$\langle r^2(t) \rangle \approx \frac{N^2 - 1}{12} + \sum_{k=2}^{(N+1)/2} \prod_{\delta=0}^{t-1} \left( 1 + 2 \frac{H_{0, \frac{N-1}{2}}^{(s(\delta)-2)}}{H_{0, \frac{N-1}{2}}^{(s(\delta))}} \left( \frac{\pi(N-1)}{2N} \right)^2 \right) \frac{(-1)^{k+1}}{2 \sin\left(\frac{\theta_k}{2}\right)} \cot\left(\frac{\theta_k}{2}\right), \quad (19)$$

(see Appendix B for the deduction of Eq. 19). Note that if  $s$  is constant, Eq. 19 becomes Eq. 13.

In this work, we study LRIs that increase from zero to a maximum value, whose time evolution is given by

$$s(t) = \begin{cases} \infty & \text{if } t = 0 \\ s_\rho t^{-\zeta} & \text{if } 1 \leq t \leq \left(\frac{s_\rho}{s_\varepsilon}\right)^{1/\zeta}, \\ s_\varepsilon & \text{otherwise} \end{cases}, \quad (20)$$

for  $s_\rho \geq s_\varepsilon$ . Due to our Markovian framework, note that  $t$  only takes integer values. For the sake of simplicity, in this work we consider  $s_\varepsilon = 1$ . Under the prior conditions, the time-evolution of MSD (on log-log scale) can be fitted to a generalized logistic curve [29]:

$$\log_{10} \langle r^2(t) \rangle \approx A_i + \frac{\log_{10} \langle r^2 \rangle_{\text{sat}} - A_i}{(1 + P_i \exp(-B_i \log_{10} t))^{\frac{1}{\nu_i}}}, \quad (21)$$

where  $A_i$ ,  $B_i$ ,  $P_i$  and  $\nu_i$  are constant parameters that depend on  $N$ ,  $s_\rho$  and  $\zeta$ , respectively. In Fig. 3, we show the time evolution of the MSD for various cycle graphs and different time-dependent LRIs, and the results of the curve fitting.

The results can be re-scaled in such a way to collapse all the curves in Fig. 3. To this purpose, we reorder the terms of Eq. 21 as follows:

$$\Theta_i \equiv \left( \frac{\log_{10} \langle r^2(t) \rangle - A_i}{\log_{10} \langle r^2 \rangle_{\text{sat}} - A_i} \right)^{\nu_i} = \frac{1}{1 + x_i}, \quad (22)$$

where  $x_i \equiv P_i t^{\frac{-B_i}{\log 10}}$ . The collapses obtained for the numerical data in Fig. 3 can be observed in Fig. 4.

According to Eq. 21 and using the Taylor series expansion of the exponential function, it is possible to observe that the time-evolution of  $\langle r^2(t) \rangle$  grows following a power-law with exponent  $\gamma = \frac{B_i (\log_{10} \langle r^2 \rangle_{\text{sat}} - A_i)}{P_i^{\frac{1}{\nu_i}} \nu_i}$ , which yields:

$$\begin{aligned} \log_{10} \langle r^2(t) \rangle &\approx A_i + \frac{\log_{10} \langle r^2 \rangle_{\text{sat}} - A_i}{P_i^{\frac{1}{\nu_i}}} \exp(B_i \log_{10} t) \approx \\ &\approx \left( A_i + \frac{\log_{10} \langle r^2 \rangle_{\text{sat}} - A_i}{P_i^{\frac{1}{\nu_i}}} \right) + \frac{B_i (\log_{10} \langle r^2 \rangle_{\text{sat}} - A_i)}{P_i^{\frac{1}{\nu_i}} \nu_i} \log_{10} t, \end{aligned} \quad (23)$$

when  $t \ll 10^{\frac{\log P_i}{B_i}}$  (i.e.,  $x_i \gg 1$ ) and the values of  $\log_{10} t$  are small.

Note that the power-law approximation expressed by Eq. 23 lasts for a finite time interval. Indeed, it shows that the exponent  $\gamma$  and the duration of this regime,  $t^*$ , depend on  $N$ ,  $s_\rho$  and  $\zeta$ , respectively, and so does the emergence of superdiffusion (i.e.,  $\gamma > 1$ ). To illustrate this dependence, in Fig 5 we show the derivative of  $\log_{10} \langle r^2(t) \rangle$  with respect to  $\log_{10} t$  for the data in Fig. 3. As can be observed in Fig. 5a, the derivative can be considered constant and equal to 1.1 in the range  $0 \leq \log_{10} t \lesssim 1.2$ . Consequently, in that region, it is possible to fit a power-law growth with exponent  $\gamma \approx 1.1$ , and it confirms the existence of a superdiffusive behaviour of MSD.

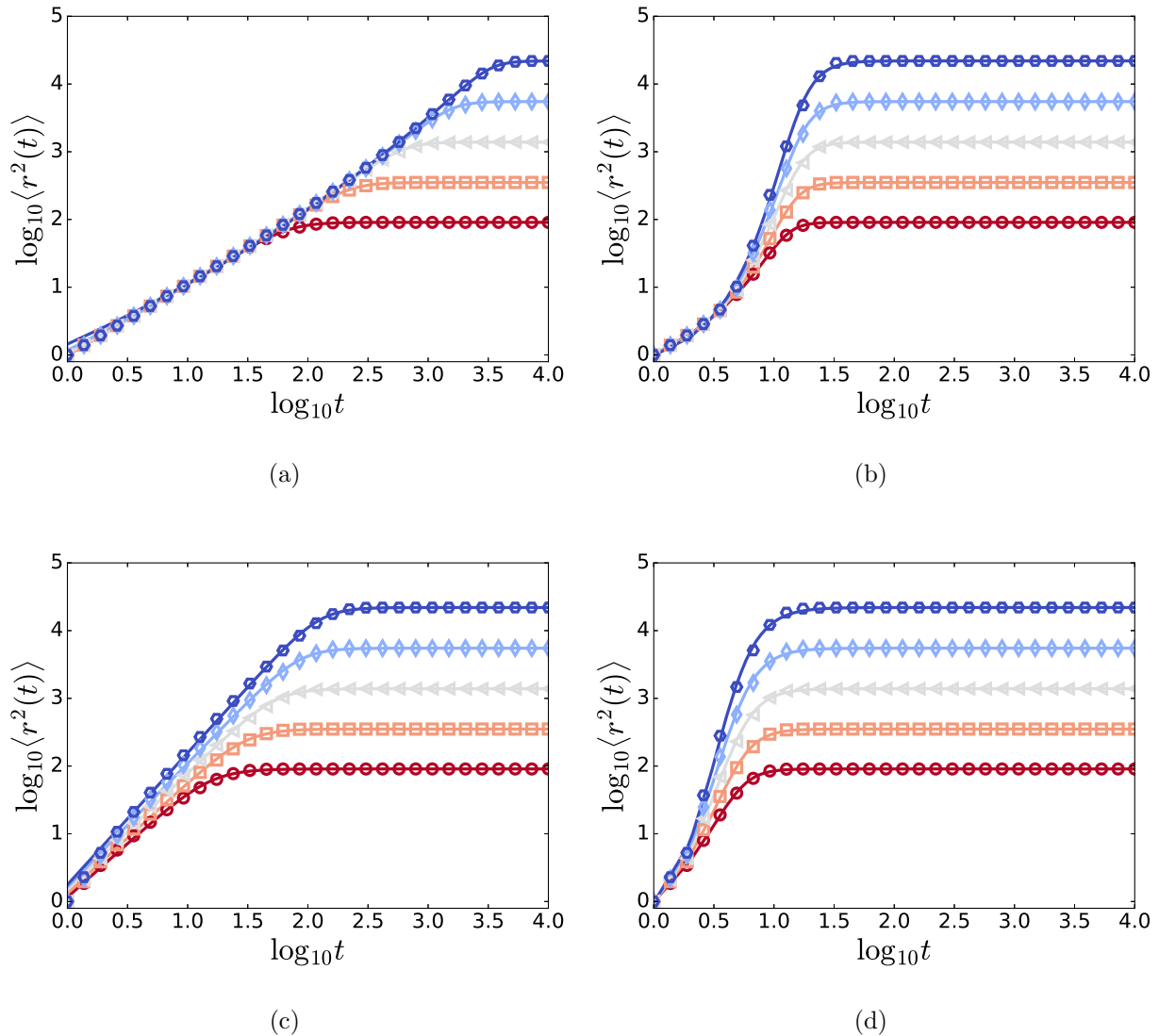


FIG. 3: Time evolution of the MSD for a cycle graph when  $N = 33$  (red circles),  $N = 65$  (orange squares),  $N = 129$  (grey triangles),  $N = 257$  (cyan rhombuses) and  $N = 513$  nodes (blue hexagons), when  $\alpha = 1.5$ . In every panel, the markers indicate the result of numerical calculation of Eq. 11, whereas the curves indicate the fitted generalized logistic curves. (a)  $\zeta = 0.1$  and  $s_\varrho = 6$ . (b)  $\zeta = 0.5$  and  $s_\varrho = 6$ . (c)  $\zeta = 0.1$  and  $s_\varrho = 3$ . (d)  $\zeta = 0.5$  and  $s_\varrho = 3$ .

On the other hand, in Fig. 5d, we show that it is possible to fit a power-law growth with exponent  $\gamma > 1$  for each series, in the range  $0 \leq \log_{10} t \lesssim 0.3$ . However, since this regime only lasts for approximately 2 time units, the superdiffusive behavior for MSD could be considered only incipient.

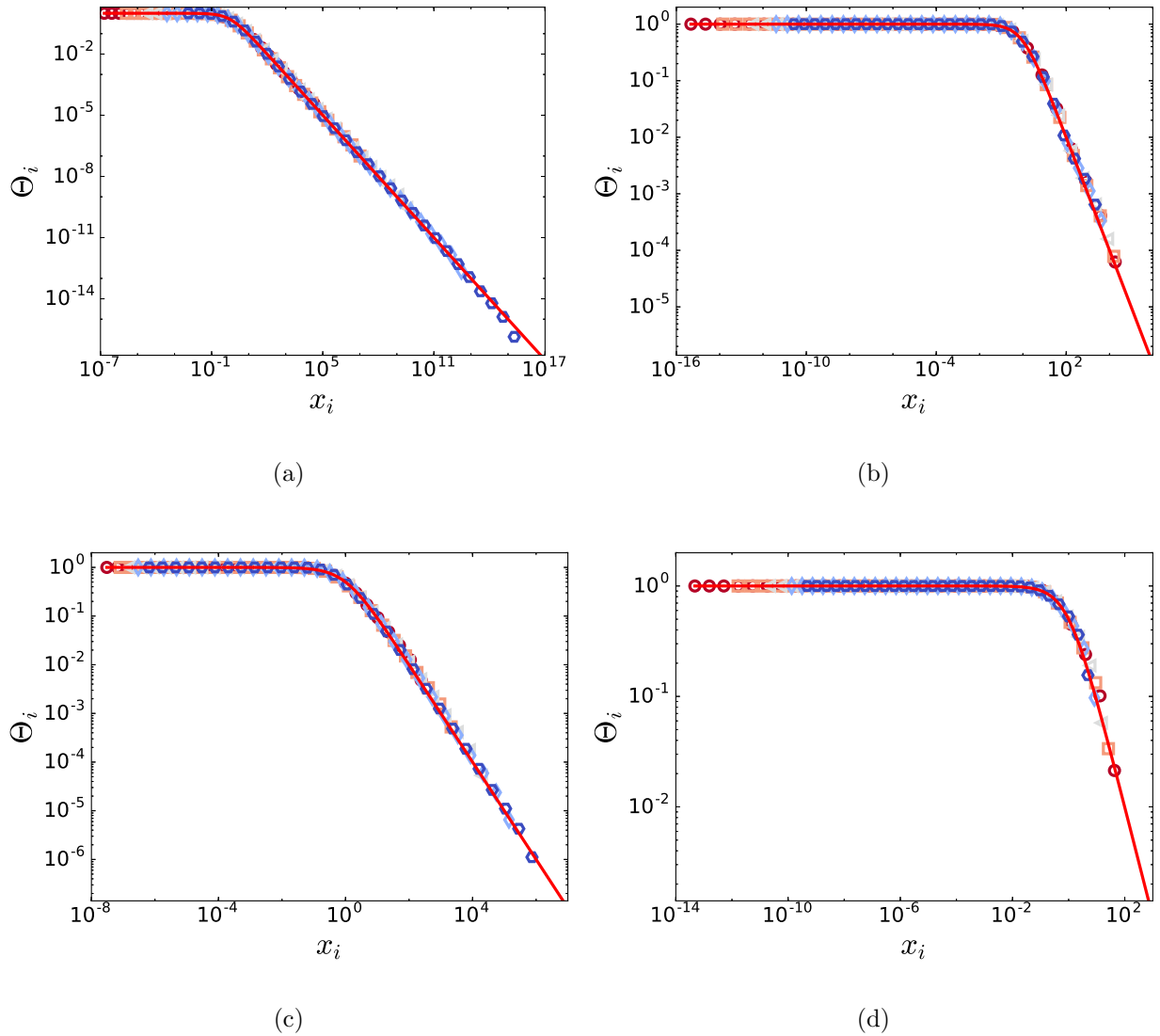


FIG. 4: The results for Eq. 22 (red continuous line) and the collapse of the results for MSD in (a) Fig. 3a, (b) Fig. 3b, (c) Fig. 3c, and (d) Fig. 3d. The symbols are the same as in the referenced figures.

### A. The exponent of the power-law regime.

We are interested in the conditions that allow the appearance of superdiffusion in these systems. Consequently, in this subsection, we explore the dependence of  $\gamma$  on  $N$ ,  $s_\rho$  and  $\zeta$ , respectively. The preliminary data for several values of  $N$ , when  $\zeta = 0.1, 0.5$  and  $s_\rho = 3, 6$  (see Fig. 5) indicate that the smaller the value of  $N$ , the smaller the initial value of  $\gamma$ , for any given  $s_\rho$ .

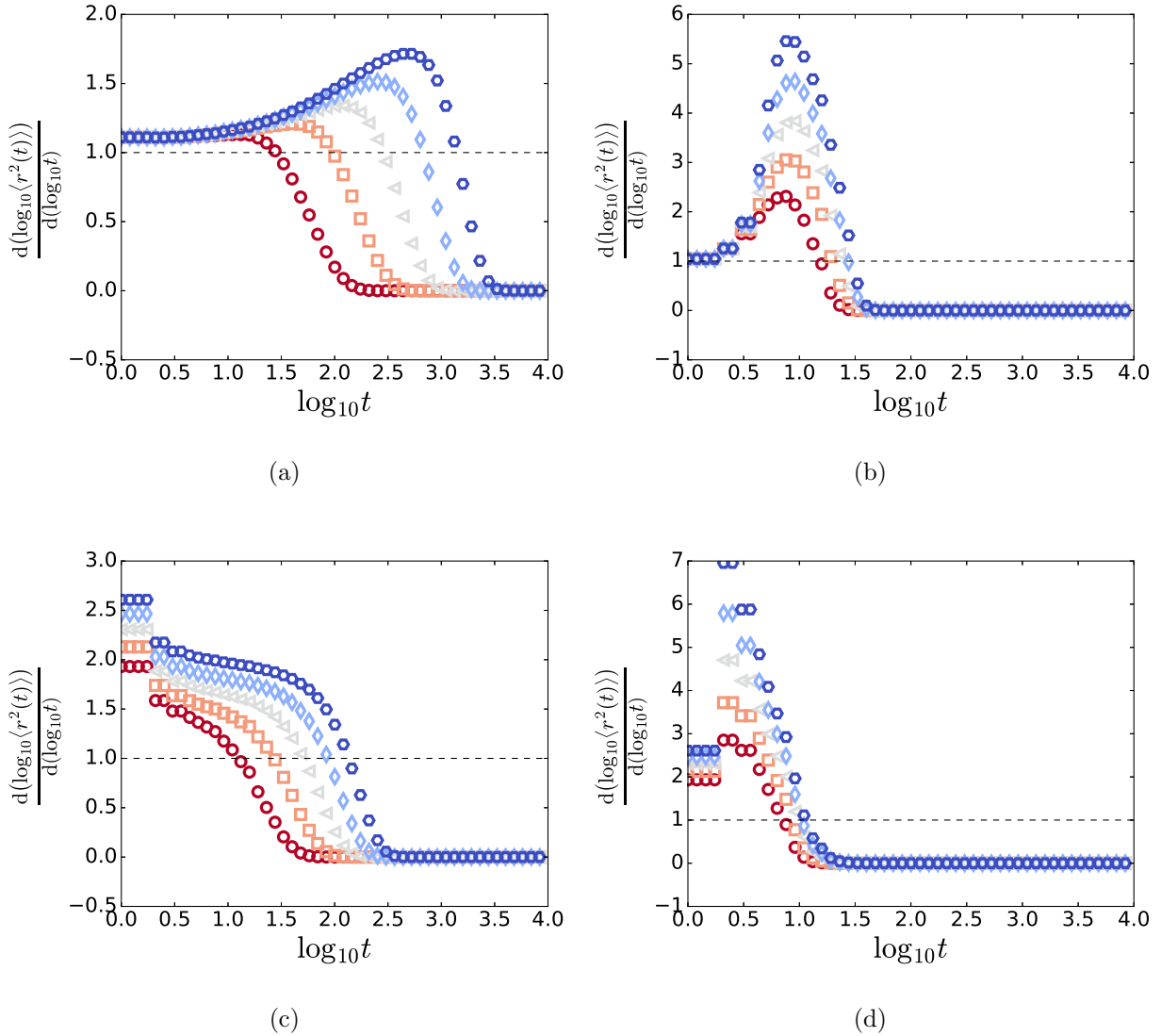


FIG. 5: The results for the derivative of  $\log_{10} \langle r^2(t) \rangle$  with respect to  $\log_{10} t$  obtained for the series in (a) Fig. 3a, (b) Fig. 3b, (c) Fig. 3c, and (d) Fig. 3d. The symbols are the same as in the referenced figures.

To clarify the dependence of  $\gamma$  on  $s_\rho$  and  $\zeta$ , we study the time evolution of the MSD for various  $s_\rho$ , when the values of  $N$  and  $\zeta$  are maintained fixed. As can be seen in Fig. 6, the smaller the value of  $s_\rho$ , the larger the initial value of  $\gamma$ , for any given  $N$ .

On the other hand, we also analyze the time evolution of the MSD for various  $\zeta$ , when the values of  $N$  and  $s_\rho$  are maintained fixed. As can be observed in Fig. 7, our numerical findings show that  $\gamma$  does not depend significantly on the value of  $\zeta$ .

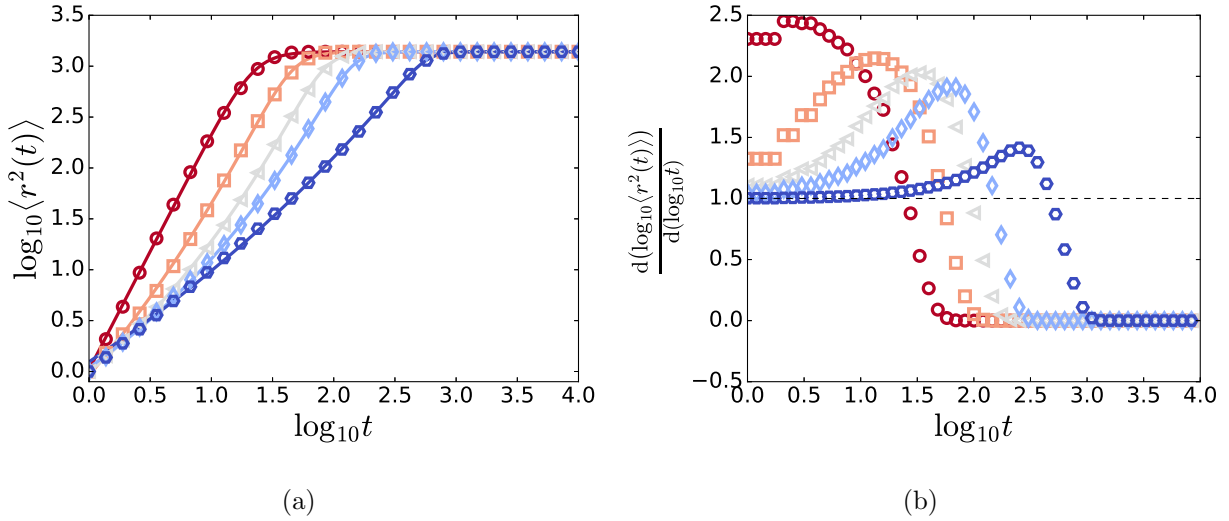


FIG. 6: (a) Left panel: Time evolution of the MSD for a cycle graph with  $N = 129$  nodes,  $s_\rho = 3$  (red circles),  $s_\rho = 4$  (orange squares),  $s_\rho = 5$  (grey triangles),  $s_\rho = 6$  (cyan rhombuses) and  $s_\rho = 10$  (blue hexagons), when  $\zeta = 0.2$  and  $\alpha = 1.5$ . The markers indicate the result of numerical calculation of Eq. 11, whereas the curves indicate the fitted generalized logistic curves. (b) Right panel: The results for the derivative of  $\log_{10} \langle r^2(t) \rangle$  with respect to  $\log_{10} t$ , for the series in Fig. 6a. The symbols are the same as in Fig. 6a.

To confirm the prior behavior, we estimate the value of  $\gamma$  as follows:

$$\gamma \approx \left( \frac{\partial \log_{10} \langle r^2(t) \rangle}{\partial \log_{10} t} \right)_{t=1} \approx \frac{\log_{10} \langle r^2(2) \rangle - \log_{10} \langle r^2(1) \rangle}{\log_{10} 2 - \log_{10} 1} \quad (24)$$

According to the time evolution of  $s(t)$  defined by Eq. 20,  $\langle r^2(1) \rangle = 1$  and  $\langle r^2(2) \rangle$  is given by:

$$\langle r^2(2) \rangle = \frac{1}{2H_{0, \frac{N-1}{2}}^{(s_\rho)}} \left\{ \frac{1}{2^{s_\rho}} + \left( \frac{N-1}{2} \right)^{2-s_\rho} + \frac{\left( \frac{N-1}{2} \right)^2}{\left( \frac{N-3}{2} \right)^{s_\rho}} + \sum_{k=1}^{(N-5)/2} (k+1)^2 \left( \frac{1}{k^{s_\rho}} + \frac{1}{(k+2)^{s_\rho}} \right) \right\}, \quad (25)$$

(see Appendix B for the deduction of Eq. 25). Note that Eq. 25 does not depend on  $\zeta$ . Therefore, the exponent  $\gamma$  of the power-law regime can be approximated by:

$$\gamma \approx \frac{\log_{10} \langle r^2(2) \rangle}{\log_{10} 2}. \quad (26)$$

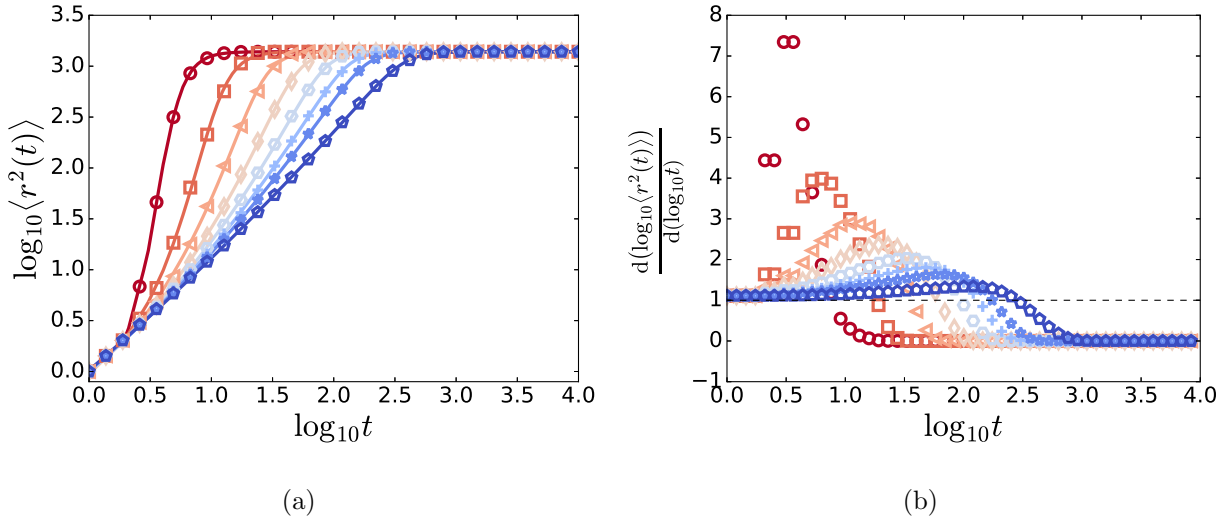


FIG. 7: (a) Left panel: Time evolution of the MSD for a cycle graph with  $N = 129$  nodes,  $\zeta = 1.0$  (circles),  $\zeta = 0.5$  (squares),  $\zeta = 0.33$  (triangles),  $\zeta = 0.25$  (rhombuses),  $\zeta = 0.20$  (hexagons),  $\zeta = 0.17$  (pluses),  $\zeta = 0.14$  (stars), and  $\zeta = 0.10$  (pentagons), when  $s_\varrho = 5$  and  $\alpha = 1.5$ . The markers indicate the result of numerical calculation of Eq. 11, whereas the curves indicate the fitted generalized logistic curves. (b) Right panel: The results for the derivative of  $\log_{10}\langle r^2(t) \rangle$  with respect to  $\log_{10}t$ , for the series in Fig. 7a. The symbols are the same as in Fig. 7a.

As can be observed in Fig. 8, our estimation confirms the numerical results observed: the smaller the value of  $s_\varrho$ , the larger the initial value of  $\gamma$ , for a given  $N$ , and the smaller the value of  $N$ , the smaller the initial value of  $\gamma$ , for a given  $s_\varrho$  (for  $s_\varrho \lesssim 4$ , otherwise the differences on  $\gamma$  are not perceptible). In the case of  $s_\varrho \gtrsim 7$ ,  $\gamma \approx 1$  (i.e., a normal diffusion takes place).

### B. The duration of the power-law regime.

If superdiffusion takes place, it lasts for a finite time interval (see Eq. 23). In order to study the conditions that allow the emergence of a lasting superdiffusive behavior, in this subsection we analyze the dependence of the power-law regime duration,  $t^*$ , on  $N$ ,  $s_\varrho$  and  $\zeta$ . As can be observed in Figs. 3, 5, 6 and 7, the numerical results suggest that  $t^*$  depends on all the previous parameters. They also indicate that  $t^*$  is proportional to the value of

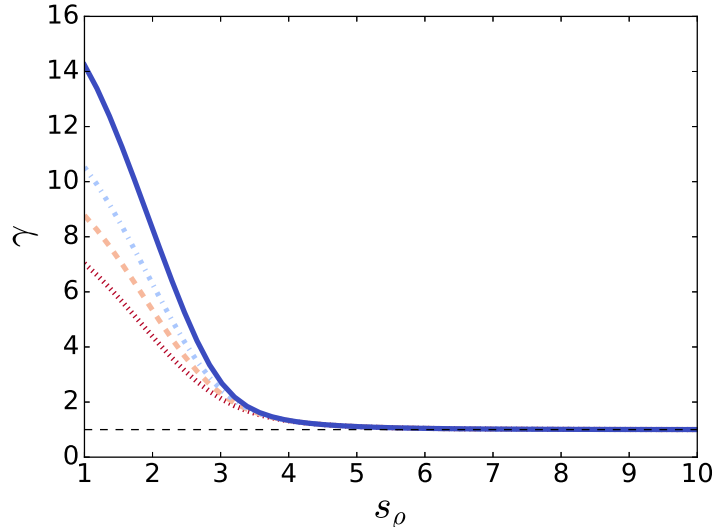


FIG. 8: Results for the dependence of  $\gamma$  on  $s_\varrho$  (using Eq. 26) for a cycle graph with  $N = 65$  nodes (red dotted line),  $N = 129$  nodes (orange dashed line),  $N = 257$  nodes (cyan dot-dashed line) and  $N = 1025$  nodes (blue solid line), when  $\alpha = 1.5$ .

$t$  where the partial derivative of  $\log_{10} \langle r^2(t) \rangle$  with respect to  $\log_{10} t$  reaches its maximum,  $t_{\max}$ . For this reason, we study the dependence of  $\log_{10} t_{\max}$  on  $N$ ,  $s_\alpha$  and  $\zeta$ .

As can be observed in Fig. 9, for a given  $N$  and  $s_\varrho$ , there is a value of  $\zeta$  that maximizes  $\log_{10} t_{\max}$ . It makes sense because, on the one hand, if  $\zeta$  is very large, MSD reaches its saturation very fast and, consequently,  $t_{\max}$  is very small. On the other hand, if  $\zeta$  is very small, then  $s(t)$  can be considered almost constant (for  $t \geq 1$ ). According to the results for constant  $s$ , the maximum value of  $\gamma$  is reached at  $t_{\max} = 1$ . Therefore, when  $\zeta$  is very small,  $t_{\max} \approx 1$ .

As can be seen in Fig. 9, given a value of  $N$ , the larger  $s_\varrho$ , the larger the maximum value of  $\log_{10} t_{\max}$ . Additionally, it is possible to observe that the value of  $\zeta$  that maximizes  $\log_{10} t_{\max}$ ,  $\zeta_{\max}$ , depends on  $s_\varrho$  and  $N$ . For a given  $N$ ,  $\zeta_{\max}$  is smaller when  $4 \lesssim s_\varrho \lesssim 6$ . On the other hand, for a given  $s_\varrho$ , the larger the value of  $N$  the smaller the  $\zeta_{\max}$ .

## VI. CONCLUSIONS

In this work, we have introduced the concept of time-dependent LRIs or time-dependent  $d$ -path transformations. We have also developed a formalism to estimate the MSD on these

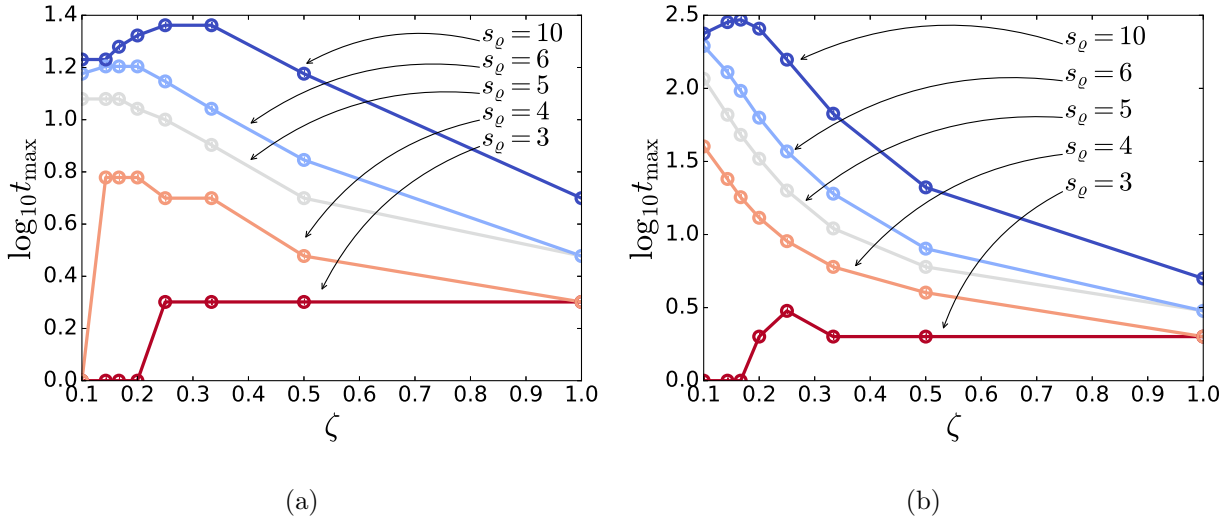


FIG. 9: Numerical results for the dependence of  $\log_{10} t_{\max}$  on  $N$  and  $\zeta$ , when  $s_{\rho} = 3, 4, 5, 6$  and 10, and  $\alpha = 1.5$ . (a) Left panel:  $N = 33$ . (b) Right panel:  $N = 129$ .

networks. To do so, we have extended the random-walk framework in [15, 23], and we have generalized the estimation of the MSD to weighted networks. As it has been shown, the MSD on networks with LRIs depends on several factors: the discrete time-step  $t$ , the  $d$ -path transformation used  $\tau$  (Mellin or Laplace), the weight of the  $d$ -path transformation ( $s$  or  $\lambda$ ), the topology of the network, and the tuning parameter of the shortest path length,  $\alpha$ . When the LRIs depend on time, the MSD is also conditioned by the time evolution of the weight of the  $d$ -path transformation ( $s(t)$  or  $\lambda(t)$ ).

To have a more clear picture of the role played by time-dependent LRIs, our approach has been specifically adapted to cycle graphs. This choice avoids the typical fast saturation of the MSD, and, additionally, it also has allowed us to derive analytical expressions for several dynamical features of the process, when constant LRIs and time-dependent ones are studied. We have considered, without loss of generality, the case of  $\tau = \text{Mellin}$  and  $\alpha \geq 1$ .

Our findings show that a rich diffusive pattern emerges when time-dependent LRIs are taken into account. In the case of constant (or even absent) LRIs, our numerical and analytical results show that the MSD on finite cycle graphs exhibits a normal diffusion ( $\gamma = 1$ ), before saturation takes place. In fact, an universal curve for the MSD evolution has been obtained.

However, in this work, we also have shown that superdiffusion can appear when the LRIs

increase with time. Specifically, when the exponent of the Mellin transformation decays from  $s(1) = s_\varrho$  to 1, following a power law with exponent  $\zeta$  (see Eq. 20), the time-evolution of MSD can be approximated by a power law for a finite time interval (see Eq. 23). The exponent and the duration of this power-law regime,  $\gamma$  and  $t^*$ , respectively, depend on  $N$  (i.e., the number of nodes),  $s_\varrho$  and  $\zeta$ . For a given  $N$ , the smaller the value of  $s_\varrho$ , the larger the exponent  $\gamma$ , and the smaller the duration  $t^*$ . On the other hand, for a given  $N$  and  $s_\varrho$ , there is a value of  $\zeta$ ,  $\zeta_{\max}$ , that maximizes the duration of the power-law behavior. Our numerical findings show that, for a given  $s_\varrho$ , the larger the value of  $N$ , the smaller the value of  $\zeta_{\max}$ . Additionally, for a given  $N$ ,  $\zeta_{\max}$  is smaller when  $4 \lesssim s_\varrho \lesssim 6$ . Taking into account these general remarks and all the results presented in this work, we conclude that it is possible to observe a significant superdiffusive behaviour on cycle graphs (i.e.,  $\gamma > 1$ ) when  $4 \lesssim s_\varrho \lesssim 6$  and  $0 < \zeta \ll 1/\log_{10} N$ .

Preliminary investigations of the same system defined on medium-sized (connected) Watts-Strogatz networks and balanced tree graphs have led to qualitatively similar results to those obtained for the cycle graphs. Of course these systems are hardly amenable to exact analytical approaches, so that a thorough investigation must heavily rely on very large size samples. Thus, given the wide applicability of the (constant or time-dependent)  $d$ -path transformations to networked systems, this work constitutes the first step toward a better understanding of diffusion on top of complex networks.

## ACKNOWLEDGMENTS

This work was supported by the project MTM2015-63914-P from the Ministry of Economy and Competitiveness of Spain and by the Brazilian agencies CNPq and CAPES. RFSA also acknowledges the support of the National Institute of Science and Technology for Complex Systems (INCT-SC Brazil).

## APPENDIX A: EIGENVALUE SPECTRUM OF A CIRCULANT MATRIX.

A  $N \times N$  circulant matrix  $\mathbf{C}$  takes the form

$$\mathbf{C} = \begin{pmatrix} c_0 & c_{N-1} & \cdots & c_2 & c_1 \\ c_1 & c_0 & c_{N-1} & & \\ \vdots & c_1 & c_0 & \ddots & \vdots \\ c_{N-2} & & \ddots & \ddots & c_{N-1} \\ c_{N-1} & c_{N-2} & \cdots & c_1 & c_0 \end{pmatrix}. \quad (27)$$

A circulant matrix  $\mathbf{C}$  is fully specified by one vector,  $\vec{c}$ , which appears as the first column of  $\mathbf{C}$ . The remaining columns of  $\mathbf{C}$  are each cyclic permutations of the vector  $\vec{c}$  with offset equal to the column index.

The normalized eigenvectors of a circulant matrix are given by:

$$\vec{v}_j = \frac{1}{\sqrt{N}} \left( 1 \ \omega_j \ \omega_j^2 \ \cdots \ \omega_j^{N-1} \right)^T, \quad (28)$$

for  $j = 0, 1, \dots, N-1$ , where

$$\omega_j = \exp\left(\mathbf{i} \frac{2\pi j}{N}\right), \quad (29)$$

are the  $N$ -th roots of unity and  $\mathbf{i}$  is the imaginary unit.

The corresponding eigenvalues are then given by:

$$\sigma_j^{\mathbf{C}} = c_0 + \sum_{k=1}^{N-1} c_k \omega_j^{N-k}, \quad (30)$$

for  $j = 0, 1, \dots, N-1$ .

## APPENDIX B: ANALYTICAL EXPRESSIONS FOR MSD ON CYCLE GRAPHS WITH TIME-DEPENDENT LRIS.

Let  $C = (V, E)$  be a simple, undirected cycle graph without self-loops and let the parameters of the Mellin and Laplace transformations depend on time (i.e.,  $s = s(t)$  and  $\lambda = \lambda(t)$ ). Then, the transformed  $d$ -path adjacency matrices of  $C$ ,  $\hat{\mathbf{A}}_t^d$ , are circulant matrices for every  $t$  (see Appendix A).

Here are two immediate consequence of the above fact:

- (i) The strength of a given node of a transformed  $d$ -path graph, at time  $t$ ,  $\hat{s}_t^\tau(i)$  does not depend on the node  $i$  (i.e.,  $\hat{s}_t^\tau(i) = \hat{s}_t^\tau$ ).
- (ii) The transition matrix for the random walk, at time  $t$ , is symmetric:

$$\mathcal{P}_t = \mathcal{P}_t^T = \frac{1}{\hat{s}_t^\tau} \hat{\mathbf{A}}_t^\tau. \quad (31)$$

All circulant matrices are diagonalized in the Fourier basis:

$$\hat{\mathbf{A}}_t^\tau = \mathbf{U} \mathbf{D}_t \mathbf{U}^*, \quad (32)$$

where  $\mathbf{U}$  is the unitary discrete Fourier transform matrix,  $\mathbf{U}^*$  is its conjugate transpose and  $D_t$  is the diagonal matrix of eigenvalues of  $\hat{\mathbf{A}}_t^\tau$ , at time  $t$ . Consequently, Eq. 7 can be expressed as follows:

$$\vec{p}_{t,i} = \left( \prod_{\delta=0}^{t-1} \mathcal{P}_\delta^T \right) \vec{p}_{0,i} = \mathbf{U} \left( \prod_{\delta=0}^{t-1} \frac{1}{\hat{s}_\delta^\tau} \mathbf{D}_\delta \right) \mathbf{U}^* \vec{p}_{0,i} = \mathbf{U} \mathbf{D}_{t-1} \mathbf{U}^* \vec{p}_{0,i}, \quad (33)$$

where

$$\mathcal{D}_{t-1}(i, i) = \frac{\prod_{\delta=0}^{t-1} \sigma_{i-1,\delta}^\tau}{\prod_{\delta=0}^{t-1} \hat{s}_\delta^\tau} = \prod_{\delta=0}^{t-1} \frac{\sigma_{i-1,\delta}^\tau}{\hat{s}_\delta^\tau}, \quad (34)$$

and  $\sigma_{i-1,\delta}^\tau$  is the  $i$ th-eigenvalue of  $\hat{\mathbf{A}}_\delta^\tau$ .

If  $N$  is an odd number and  $\tau = \text{Mellin}$ , it is possible to write:

$$\sigma_{k,\delta}^{\text{Mellin}} = \sum_{d=1}^{(N-1)/2} \frac{1}{d^{s(\delta)}} (\omega_k^{N-d} + \omega_k^d) = \sum_{d=1}^{(N-1)/2} \frac{2}{d^{s(\delta)}} \cos\left(\frac{2\pi kd}{N}\right), \quad (35)$$

and

$$\hat{s}_\delta^{\text{Mellin}} = \sum_{d=1}^{(N-1)/2} \frac{2}{d^{s(\delta)}} = 2H_{\frac{N-1}{2}}^{(s(\delta))}, \quad (36)$$

for  $k = 0, 1, \dots, N-1$ , where  $H_n^{(m)}$  is the generalized harmonic number of order  $n$  of  $m$ ,

$$\omega_k = \exp\left(\mathbf{i} \frac{2\pi k}{N}\right), \quad (37)$$

are the  $N$ -th roots of unity, and  $\mathbf{i} = \sqrt{-1}$  (see the Appendix A). Note that  $\omega_k^N = 1$  and, consequently,  $\omega_k^{N-d} = \omega_k^{-d}$ . As can be observed, it is straightforward to obtain a similar equation for  $\tau = \text{Laplace}$ .

The unitary discrete Fourier transform matrix  $\mathbf{U}$  can be defined as:

$$\mathbf{U}(i, j) = \left( \frac{\omega_{-1}^{(i-1)(j-1)}}{\sqrt{N}} \right). \quad (38)$$

Consequently, according to Eq. 33, given an initial condition  $\vec{p}_{0,i}$ , the probability of finding a random walker at node  $q$ , at time  $t$ , is given by:

$$(\vec{p}_{t,i})_q = \sum_{j=1}^N \sum_{k=1}^N \mathbf{U}(q, k) \mathcal{D}_{t-1}(k, k) \mathbf{U}^*(k, j) (\vec{p}_{0,i})_j. \quad (39)$$

According to the topology of the cycle graphs,  $r^2(t, i) = r^2(t, j)$  for  $i \neq j$  (see Eq. 10). Therefore, using Eq. 39, if  $N$  is odd, it is possible to write Eq. 11 as follows:

$$\begin{aligned} \langle r^2(t) \rangle &= \frac{1}{N} \sum_{q=1}^N r^2(t, q) = r^2(t, i) = \sum_{q=1}^N (d_{q,i}^\alpha)^2 (\vec{p}_{t,i})_q = \\ &= \sum_{q=1}^N \sum_{j=1}^N \sum_{k=1}^N (i - q)^2 \mathbf{U}(q, k) \mathcal{D}_{t-1}(k, k) \mathbf{U}^*(k, j) (\vec{p}_{0,i})_j, \end{aligned} \quad (40)$$

for cycle graphs, when  $i = \frac{N+1}{2}$  and  $\alpha \geq 1$  (i.e.,  $(d_{q,i}^\alpha)^2 = (d_{q,i})^2 = (i - q)^2$ ). According to the definition of the vector  $\vec{p}_{0,i}$ , Eq. 40 results in:

$$\begin{aligned} \langle r^2(t) \rangle &= \sum_{q=1}^N \sum_{k=1}^N (i - q)^2 \frac{1}{N} \exp(\mathbf{i}\theta_k (i - q)) \mathcal{D}_{t-1}(k, k) = \\ &= \sum_{q=1}^N (i - q)^2 \frac{1}{N} + \sum_{q=1}^N \sum_{k=2}^N (i - q)^2 \frac{1}{N} \exp(\mathbf{i}\theta_k (i - q)) \mathcal{D}_{t-1}(k, k) = \\ &= \frac{N^2 - 1}{12} + \sum_{k=2}^N \frac{1}{N} \mathcal{D}_{t-1}(k, k) \sum_{q=1}^N (i - q)^2 \exp(\mathbf{i}\theta_k (i - q)) = \\ &= \frac{N^2 - 1}{12} + \sum_{k=2}^N \mathcal{D}_{t-1}(k, k) \frac{\exp(\mathbf{i}\theta_k i)}{\exp(\mathbf{i}\theta_k) - 1} \left( 2(i - 1) + N - \frac{2}{\exp(\mathbf{i}\theta_k) - 1} \right) = \\ &= \frac{N^2 - 1}{12} + \sum_{k=2}^N \mathcal{D}_{t-1}(k, k) \Phi(k), \end{aligned} \quad (41)$$

where we introduce the short-hand notation

$$\Phi(k) \equiv \frac{\exp(i\theta_k i)}{\exp(i\theta_k) - 1} \left( 2(i-1) + N - \frac{2}{\exp(i\theta_k) - 1} \right) = \frac{(-1)^k}{2 \sin\left(\frac{\theta_k}{2}\right)} \left( 2Ni - \cot\left(\frac{\theta_k}{2}\right) \right), \quad (42)$$

and  $\theta_k \equiv \frac{2\pi}{N}(k-1)$ , for  $i = \frac{N+1}{2}$  (see Appendix B). As can be observed, Eq. 41 includes a constant term. It can be proved that it is the saturation value of MSD on cycle graphs (see Appendix B).

Given that  $\theta_k \equiv -\theta_{N+2-k} \pmod{2\pi}$ ,  $\mathcal{D}_{t-1}(k, k) = \mathcal{D}_{t-1}(N+2-k, N+2-k)$  and  $\Phi(k) = \Phi^*(N+2-k)$ . Therefore, MSD can be expressed as:

$$\langle r^2(t) \rangle = \frac{N^2 - 1}{12} + \sum_{k=2}^{(N+1)/2} \mathcal{D}_{t-1}(k, k) \frac{(-1)^{k+1}}{2 \sin\left(\frac{\theta_k}{2}\right)} \cot\left(\frac{\theta_k}{2}\right), \quad (43)$$

on cycle graphs with an odd number of nodes.

#### A. Time evolution of the MSD on cycle graphs without LRIs

In case of  $s = \infty$  for every  $t$ ,  $\mathcal{D}_{t-1}(k, k) = \cos^t(\theta_k)$ . Thus, according to Eq. 43, MSD is given by:

$$\langle r^2(t) \rangle = \frac{N^2 - 1}{12} + \sum_{k=2}^{(N+1)/2} \cos^t(\theta_k) \frac{(-1)^{k+1}}{2 \sin\left(\frac{\theta_k}{2}\right)} \cot\left(\frac{\theta_k}{2}\right). \quad (44)$$

#### B. Time evolution of the MSD on cycle graphs with constant LRIs

In case of  $s = 0$  for every  $t$ , we obtain the following result:

$$\mathcal{D}_{t-1}(k, k) = \left( \frac{2}{N-1} \csc\left(\frac{\theta_t}{2}\right) \sin\left(\frac{\theta_t(N-1)}{4}\right) \cos\left(\frac{\theta_t(N+1)}{4}\right) \right)^t. \quad (45)$$

Generally, in case of constant  $s$ , taking into account that  $d/N < 0.5$ , Eq. 35 can be written as follows:

$$\begin{aligned} \sigma_{k,\delta}^{\text{Mellin}} &= \sum_{d=1}^{(N-1)/2} \frac{2}{d^s} \cos\left(\frac{2\pi kd}{N}\right) \approx \sum_{d=1}^{(N-1)/2} \frac{2}{d^s} \left( 1 + \frac{1}{2} \left( \frac{2\pi kd}{N} \right)^2 \right) = \\ &= 2H_{\frac{N-1}{2}}^{(s)} + \left( \frac{2\pi k}{N} \right)^2 H_{\frac{N-1}{2}}^{(s-2)}. \end{aligned} \quad (46)$$

Thus, Eqs. 34 and 43 can be expressed as

$$\mathcal{D}_{t-1}(i, i) = \prod_{\delta=0}^{t-1} \frac{\sigma_{i-1, \delta}^{\tau}}{\hat{\sigma}_{\delta}^{\tau}} \approx \left( 1 + 2 \frac{H_{\frac{N-1}{2}}^{(s-2)}}{H_{\frac{N-1}{2}}^{(s)}} \left( \frac{\pi(i-1)}{N} \right)^2 \right)^t, \quad (47)$$

and

$$\langle r^2(t) \rangle \approx \frac{N^2 - 1}{12} + \sum_{k=2}^{(N+1)/2} \left( 1 + 2 \frac{H_{\frac{N-1}{2}}^{(s-2)}}{H_{\frac{N-1}{2}}^{(s)}} \left( \frac{\pi(i-1)}{N} \right)^2 \right)^t \frac{(-1)^{k+1}}{2 \sin \left( \frac{\theta_k}{2} \right)} \cot \left( \frac{\theta_k}{2} \right). \quad (48)$$

### C. Time evolution of the MSD on cycle graphs with time-dependent LRIs

Generally, taking into account that  $d/N < 0.5$ , Eq. 35 can be written as follows:

$$\begin{aligned} \sigma_{k, \delta}^{\text{Mellin}} &= \sum_{d=1}^{(N-1)/2} \frac{2}{d^{s(\delta)}} \cos \left( \frac{2\pi kd}{N} \right) \approx \sum_{d=1}^{(N-1)/2} \frac{2}{d^{s(\delta)}} \left( 1 + \frac{1}{2} \left( \frac{2\pi kd}{N} \right)^2 \right) = \\ &= 2H_{\frac{N-1}{2}}^{(s(\delta))} + \left( \frac{2\pi k}{N} \right)^2 H_{\frac{N-1}{2}}^{(s(\delta)-2)}. \end{aligned} \quad (49)$$

Thus, Eqs. 34 and 43 can be expressed as:

$$\mathcal{D}_{t-1}(i, i) = \prod_{\delta=0}^{t-1} \frac{\sigma_{i-1, \delta}^{\tau}}{\hat{\sigma}_{\delta}^{\tau}} \approx \prod_{\delta=0}^{t-1} \left( 1 + 2 \frac{H_{\frac{N-1}{2}}^{(s(\delta)-2)}}{H_{\frac{N-1}{2}}^{(s(\delta))}} \left( \frac{\pi(i-1)}{N} \right)^2 \right), \quad (50)$$

and

$$\langle r^2(t) \rangle \approx \frac{N^2 - 1}{12} + \sum_{k=2}^{(N+1)/2} \prod_{\delta=0}^{t-1} \left( 1 + 2 \frac{H_{\frac{N-1}{2}}^{(s(\delta)-2)}}{H_{\frac{N-1}{2}}^{(s(\delta))}} \left( \frac{\pi(i-1)}{N} \right)^2 \right) \frac{(-1)^{k+1}}{2 \sin \left( \frac{\theta_k}{2} \right)} \cot \left( \frac{\theta_k}{2} \right). \quad (51)$$

### D. Operations on Eq. 41.

To simplify the right hand term of Eq. 41, we proceed as follows:

$$\begin{aligned} &\sum_{k=2}^N \frac{1}{N} \mathcal{D}_{t-1}(k, k) \sum_{q=1}^N (i-q)^2 \exp(i\theta_k(i-q)) = \\ &\sum_{k=2}^N \frac{1}{N} \mathcal{D}_{t-1}(k, k) \frac{1}{(i\theta_k)^2} \sum_{q=1}^N (i\theta_k(i-q))^2 \exp(i\theta_k(i-q)). \end{aligned} \quad (52)$$

The summation on  $q$  of Eq. 52 results in:

$$\begin{aligned}
\sum_{q=1}^N (\mathbf{i}\theta_k (i-q))^2 \exp(\mathbf{i}\theta_k (i-q)) &= \sum_{q=1}^N \frac{\partial^2}{\partial a^2} [\exp(\mathbf{i}\theta_k (i-q) a)]_{a=1} = \\
&= \frac{\partial^2}{\partial a^2} \left[ \exp(\mathbf{i}\theta_k i a) \sum_{q=1}^N (\exp(-\mathbf{i}\theta_k a))^q \right]_{a=1} = \\
&= \frac{\partial^2}{\partial a^2} \left[ \exp(\mathbf{i}\theta_k (i-1) a) \frac{1 - \exp(-\mathbf{i}\theta_k a N)}{1 - \exp(-\mathbf{i}\theta_k a)} \right]_{a=1} = \\
&= N (\mathbf{i}\theta_k)^2 \exp(\mathbf{i}\theta_k i) \left( \frac{(i-1)^2 (1 - \exp(-\mathbf{i}\theta_k N))}{N (\exp(\mathbf{i}\theta_k) - 1)} - \frac{2(i-1) (1 - \exp(-\mathbf{i}\theta_k N))}{N (\exp(\mathbf{i}\theta_k) - 1)^2} + \right. \\
&\quad \left. + \frac{2(i-1) \exp(-\mathbf{i}\theta_k N)}{\exp(\mathbf{i}\theta_k) - 1} + \frac{N \exp(-\mathbf{i}\theta_k N)}{\exp(\mathbf{i}\theta_k) - 1} + \right. \\
&\quad \left. + \frac{(\exp(\mathbf{i}\theta_k) + 1) (1 - \exp(-\mathbf{i}\theta_k N))}{N (\exp(\mathbf{i}\theta_k) - 1)^3} - \frac{2 \exp(-\mathbf{i}\theta_k N)}{(\exp(\mathbf{i}\theta_k) - 1)^2} \right). \tag{53}
\end{aligned}$$

Finally, taking into account that  $\exp(\mathbf{i}\theta_k N) = \exp(-\mathbf{i}\theta_k N) = 1$ , we obtain the result presented in Eq. 41.

### E. Saturation value of MSD on cycle graphs

If  $k \geq 2$  and  $s(t) > 0$ , according to Eqs. 35 and 36,  $\sigma_{k-1,t}^{\text{Mellin}} < \hat{s}_t^{\text{Mellin}}$ , for  $t \geq 0$ . Let  $r$  be the maximum value of  $\sigma_{k-1,t}^{\text{Mellin}} / \hat{s}_t^{\text{Mellin}}$ . Then, it is possible to proof that the following limit tend to zero:

$$\begin{aligned}
&\lim_{t \rightarrow \infty} \sum_{k=2}^N \mathcal{D}_{t-1}(k, k) \frac{\exp(\mathbf{i}\theta_k i)}{\exp(\mathbf{i}\theta_k) - 1} \left( 2(i-1) + N - \frac{2}{\exp(\mathbf{i}\theta_k) - 1} \right) = \\
&\sum_{k=2}^N \left( \lim_{t \rightarrow \infty} \prod_{\delta=0}^{t-1} \frac{\sigma_{k-1,\delta}^{\text{Mellin}}}{\hat{s}_\delta^{\text{Mellin}}} \right) \frac{\exp(\mathbf{i}\theta_k i)}{\exp(\mathbf{i}\theta_k) - 1} \left( 2(i-1) + N - \frac{2}{\exp(\mathbf{i}\theta_k) - 1} \right) < \\
&< \sum_{k=2}^N \left( \lim_{t \rightarrow \infty} \prod_{\delta=0}^{t-1} r \right) \frac{\exp(\mathbf{i}\theta_k i)}{\exp(\mathbf{i}\theta_k) - 1} \left( 2(i-1) + N - \frac{2}{\exp(\mathbf{i}\theta_k) - 1} \right) = \\
&= \sum_{k=2}^N \left( \lim_{t \rightarrow \infty} r^t \right) \frac{\exp(\mathbf{i}\theta_k i)}{\exp(\mathbf{i}\theta_k) - 1} \left( 2(i-1) + N - \frac{2}{\exp(\mathbf{i}\theta_k) - 1} \right) = 0. \tag{54}
\end{aligned}$$

Consequently, according to Eq. 41, we obtain:

$$\lim_{t \rightarrow \infty} \langle r^2(t) \rangle = \frac{N^2 - 1}{12}. \quad (55)$$

### F. On $\Phi(k)$

According to the definition of  $\Phi(k)$  (Eq. 42), for  $i = \frac{N+1}{2}$ , it is possible to write:

$$\begin{aligned} \Phi(k) &\equiv \frac{\exp(i\theta_k i)}{\exp(i\theta_k) - 1} \left( 2(i-1) + N - \frac{2}{\exp(i\theta_k) - 1} \right) = \\ &= \exp(i\theta_k i) \frac{\exp(-i\theta_k) - 1}{2(1 - \cos(\theta_k))} \left( 2N - 1 - 2 \frac{\exp(-i\theta_k) - 1}{2(1 - \cos(\theta_k))} \right) = \\ &= \frac{\exp(i\theta_k \frac{N-1}{2}) - \exp(i\theta_k \frac{N+1}{2})}{2(1 - \cos(\theta_k))} \left( 2N - 1 - 2 \frac{\cos(\theta_k) - 1 - i \sin(\theta_k)}{2(1 - \cos(\theta_k))} \right) = \\ &= \frac{\exp(i\theta_k \frac{N}{2}) (-i) \sin(\frac{\theta_k}{2})}{2 \sin^2(\frac{\theta_k}{2})} \left( 2N + \frac{i2 \sin(\frac{\theta_k}{2}) \cos(\frac{\theta_k}{2})}{2 \sin^2(\frac{\theta_k}{2})} \right) = \\ &= \frac{\exp(i\pi k) \exp(-i\pi) (-i)}{2 \sin(\frac{\theta_k}{2})} \left( 2N + i \cot\left(\frac{\theta_k}{2}\right) \right) = \\ &= \frac{(-1)^k}{2 \sin(\frac{\theta_k}{2})} \left( 2Ni - \cot\left(\frac{\theta_k}{2}\right) \right). \end{aligned} \quad (56)$$

### G. Deduction of Eq. 25

According to the time evolution of  $s(t)$  defined by Eq. 20,  $s(0) = \infty$ . Therefore, at time  $t = 1$ , the probability of finding the random walker at node  $j$  is given by:

$$\left( \vec{p}_{1, \frac{N+1}{2}} \right)_j = \begin{cases} \frac{1}{2} & \text{if } j = \frac{N+1}{2} - 1, \frac{N+1}{2} + 1 \\ 0 & \text{otherwise} \end{cases}. \quad (57)$$

If the number of nodes  $N$  is odd, then  $\left( d_{\frac{N+1}{2}, j}^\alpha \right)^2 = \left( j - \frac{N+1}{2} \right)^2$  for  $\alpha \geq 1$ , and

$$\vec{p}_{2, \frac{N+1}{2}} = \left( \sum_{k=1}^{(N-1)/2} \frac{1}{k^{s_\alpha}} \mathbf{A}_d \right) \vec{p}_{1, \frac{N+1}{2}}, \quad (58)$$

when the Mellin transformation is used. Consequently, according to Eq. 11, at time  $t = 2$ , MSD is given by:

$$\langle r^2(2) \rangle = \sum_{j=1}^N \left( j - \frac{N+1}{2} \right)^2 \left( \vec{p}_{2, \frac{N+1}{2}} \right)_j = 2 \sum_{j=1}^{(N-1)/2} \left( j - \frac{N+1}{2} \right)^2 \left( \vec{p}_{2, \frac{N+1}{2}} \right)_j. \quad (59)$$

Conducting the necessary manipulation, Eq. 59 results in Eq. 25.

- 
- [1] E. Estrada. The Structure of Complex Networks. Theory and Applications. *Oxford Univ. Press, Oxford*, 2012.
- [2] J. D. Noh, and H. Rieger. Random walks on complex networks. *Phys. Rev. Lett.*, *92*, *11*, 118701, 2004.
- [3] J. Klafter, and I. M. Sokolov. First steps in random walks: from tools to applications. *Oxford University Press*, 2011.
- [4] M. Schunack, T. R. Linderoth, F. Rosei, E. Lægsgaard, I. Stensgaard, and F. Besenbacher. Long jumps in the surface diffusion of large molecules. *Phys. Rev. Lett.*, *88*, 156102, 2002.
- [5] C. Yu, J. Guan, K. Chen, S. Chul Bae, and S. Granick. Single-molecule observation of long jumps in polymer adsorption. *ACS nano*, *7*, 2013.
- [6] T. Ala-Nissila, R. Ferrando, and S.C. Ying. Collective and single particle diffusion on surfaces, *Advances in Physics*, *51*, pp. 949–1078., 2002.
- [7] R. Guantes, J. L. Vega, and S. Miret-Artés. Chaos and anomalous diffusion of adatoms on solid surfaces, *Phys. Rev. B*, *64*, 245415, 2001.
- [8] M. Lomholt, K. Tal, R. Metzler, and K. Joseph. Lévy strategies in intermittent search processes are advantageous, *Proceedings of the National Academy of Sciences*, *105*, *32*, 11055–11059, 2008.
- [9] N. E. Humphries, N. Queiroz, J. R. N. Dyer, N. G. Pade, M. Musyl, K. M. Schaefer, D. W. Fuller, J. M. Brunnschweiler, T. K. Doyle, J. D. R. Houghton, and others. Environmental context explains Lévy and Brownian movement patterns of marine predators, *Nature*, *465*, 7301, 1066–1066, 2010.
- [10] Song, Chaoming and Koren, Tal and Wang, Pu and Barabási, Albert-László. Modelling the scaling properties of human mobility, *Nature Physics*, *6*, *10*, 818–823, 2010
- [11] I. Rhee, M. Shin, S. Hong, K. Lee, S. J Kim, and S. Chong. On the levy-walk nature of human mobility, *IEEE/ACM transactions on networking (TON)*, *19*, *3*, 630–643, 2011.

- [12] O.G. Bakunin. Chaotic Flows, *Springer Ser. Synergetics, vol.10, Springer, Berlin, Heidelberg*, 2011.
- [13] C. Tsallis. Introduction to Nonextensive Statistical Mechanics: Approaching a Complex World *Springer, New York*, 2009.
- [14] E. Estrada. Path Laplacian matrices: Introduction and application to the analysis of consensus in networks. *Linear Algebra and its Applications* 436, 2012.
- [15] E. Estrada, J.-C. Delvenne, N. Hatano, J. L. Mateos, R. Metzler, and M. T. Schaub. Random multi-hopper model: super-fast random walks on graphs. *Journal of Complex Networks*, 2017, in press.
- [16] E. Estrada, and E. Vargas-Estrada. How peer pressure shapes consensus, leadership, and innovations in social groups. *Scientific Reports*, 3, 2013.
- [17] E. Estrada, L. Gambuzza, and M. Frasca. Long-range interactions and network synchronization. *SIAM J. Appl. Dyn. Syst.*, 2018, in press.
- [18] E. Estrada, E. Hameed, N. Hatano, and M. Langer. Path Laplacian operators and superdiffusive processes on graphs. I. One-dimensional case. *Linear Algebra and its Applications* 523, 2017.
- [19] P. Ormerod, and G. Wiltshire. “Binge” drinking in the UK: a social network phenomenon *Mind Soc.* 8, 135, 2009.
- [20] D. Aldous, and J. A. Fill. “Reversible Markov Chains and Random Walks on Graphs”, 2002.
- [21] L. Lovász. “Random walks on graphs: A Survey”, *Combinatorics, Paul Erdos Is Eighty*, 2, 1–46, 1993.
- [22] R. F. S. Andrade, J. G. V. Miranda, and T. Petit Lobão. “Neighborhood properties of complex networks”, *Phys. Rev. E* 73, 046101, 2006.
- [23] Z. Zhang, T. Shan, and G. Chen. “Random walks on weighted networks”, *Phys. Rev. E* 87, 012112, 2013.
- [24] E. Almaas, R. V. Kulkarni, and D. Stroud. “Scaling properties of random walks on small-world networks”, *Phys. Rev. E* 68, 056105, 2003.
- [25] L. K. Gallos. “Random walk and trapping processes on scale-free networks”, *Phys. Rev. E* 70, 046116, 2004.
- [26] T. Opsahl, F. Agneessens, and J. Skvoretz. “Node centrality in weighted networks: Generalizing degree and shortest paths”, *Social Networks*, 32, 245–251, 2010.

- [27] E.W. Dijkstra. “A note on two problems in connexion with graphs”, *Numerische Mathematik* **1**, 269–271, 1959.
- [28] M. J. Kronenburg. “Some generalized harmonic number identities”, arXiv: 1103.5430v2, 2012.
- [29] F. J. Richards. “A Flexible Growth Function for Empirical Use”, *Journal of Experimental Botany* **10**, Issue 2, 290–301, 1959.